# A Direct Torque Controlled Brushless Doubly-Fed Reluctance Machine Drive System

Milutin JOVANOVIĆ[1], Member, IEEE, and Jian YU[2], Member, IEEE

[1]Northumbria University, Newcastle upon Tyne, United Kingdom, e-mail: milutin.jovanovic@northumbria.ac.uk
[2]PB Power, Newcastle upon Tyne, United Kingdom, e-mail: YuJ@pbworld.com

***Abstract*— The paper proposes a viable direct torque control (DTC) scheme for limited speed range applications of the Brushless Doubly Fed Reluctance Machine (BDFRM). The simulation and experimental results generated for a small prototype will show that the machine can successfully operate down to zero supply frequency of the inverter-fed (secondary) winding, unlike cage induction or many other traditional AC machines with DTC.**

***Index Terms*—Direct Torque Control, Reluctance Drives.**

## I. Introduction

The brushless doubly fed reluctance machine (BDFRM) belongs to the slip power recovery family of machines together with the classical cascaded induction machines (CIM) and the, so called, self-cascaded (single-frame) machines including the doubly-excited wound rotor induction machine (DEWRIM) and a BDFRM cage counterpart, the brushless doubly-fed induction machine (BDFIM). All the machines from this group allow the use of a partially rated converter, which makes it possible to lower the capital cost of a drive. This is especially the case in larger power applications with restricted variable speed capability (such as pumps and wind turbines) where the converter size can be further reduced [1]. In these systems the supply quality would also be improved as less harmonics would be injected into the grid by the smaller inverter.

In comparison with the other family members, the BDFRM is superior in many respects. Its brushless structure offers higher reliability and maintenance-free operation in contrast to the DEWRIM. The BDFIM, on the other hand, uses the same double-winding stator but because of a special cage rotor [2], it should be less efficient [3] and more difficult to model and control than the BDFRM having a cageless reluctance rotor. In fact, unlike the BDFIM, vector control of the BDFRM grid-connected (primary) winding reactive power and torque is inherently decoupled [4] (so is with the DEWRIM), and therefore much simpler.

The main objective of this paper is the development and experimental evaluation of an algorithm (Fig. 1) for direct control of the secondary (inverter-fed) winding flux and electromagnetic torque, commonly referred to as Direct Torque Control (DTC), of the BDFRM. This method has been extremely popular for higher speed applications of almost all conventional AC machines but has not been seriously considered for doubly-fed drive systems so far. An alternative DTC technique, that has been proposed for the BDFIM in [5], is rotor frame based, requires the use of a shaft sensor for torque control and it is very complex and time consuming even for DSP implementation [5]. A DTC scheme recently presented in [6] for a doubly-fed variable speed wind turbine induction generator, on the other hand, has not been practically validated.

Another motivation for the work presented in the following is the prospect for faster transient response[1] that can be achieved from the machine by varying the control variables directly in a 'bang-bang' fashion. It will be shown that in terms of amenability to DTC implementation and obtainable performance, the BDFRM may be preferable to traditional machines. This is foremost related to the possibility of its operation down to zero secondary frequency. In this sense, the paper is significant and can serve as a good reference for DTC research not only on the BDFRM but also on the DEWRIM due to close modelling similarities between these two conceptually different machines.

## II. Dynamic Model

The space-vector equations in a stationary reference frame and the fundamental angular velocity relationship for the machine are [7–9]:

$$\underline{u}_p = R_p\underline{i}_p + \frac{d\underline{\lambda}_p}{dt} = R_p\underline{i}_p + \left.\frac{d\underline{\lambda}_p}{dt}\right|_{\theta_p \text{ const}} + j\omega_p\underline{\lambda}_p \quad (1)$$

$$\underline{u}_s = R_s\underline{i}_s + \frac{d\underline{\lambda}_s}{dt} = R_s\underline{i}_s + \left.\frac{d\underline{\lambda}_s}{dt}\right|_{\theta_s \text{ const}} + j\omega_s\underline{\lambda}_s \quad (2)$$

$$\underline{\lambda}_p = \lambda_p e^{j\theta_p} = L_p\underline{i}_p + L_{ps}\underline{i}_s^* e^{j\theta_r} \quad (3)$$

$$\underline{\lambda}_s = \lambda_s e^{j\theta_s} = L_s\underline{i}_s + L_{ps}\underline{i}_p^* e^{j\theta_r} \quad (4)$$

$$\omega_r = d\theta_r/dt = p_r\omega_{rm} = \omega_p + \omega_s = (1-s)\omega_p \quad (5)$$

where '*' denotes the complex conjugate, $L_{p,s,ps}$ are the 3-phase inductances of the primary and secondary windings [8, 10], $\omega_{rm}$ is the rotor mechanical angular velocity, $p_r$ is the rotor pole number, $\omega_{p,s}$ are the applied frequencies to the windings (rad/s) and $s = -\omega_s/\omega_p$ is the 'generic' slip. Notice from (5) that $\omega_s > 0$ for super-synchronous operation (when $s < 0$ as with induction generators) and $\omega_s < 0$[2] if the machine is operated below the synchronous speed[3] i.e. in

[1]Because of the unusual operating principle and the higher leakage inductances [7, 8], the BDFRM dynamic performance is generally compromised compared to conventional machines.

[2]The negative secondary frequency indicates the opposite phase sequence of the secondary winding to the primary one.

[3]The BDFRM runs at this speed if the secondary side is DC supplied i.e. when $\omega_s = s = 0$. The secondary obviously plays the role of the field winding of a classical wound rotor synchronous machine in this case.

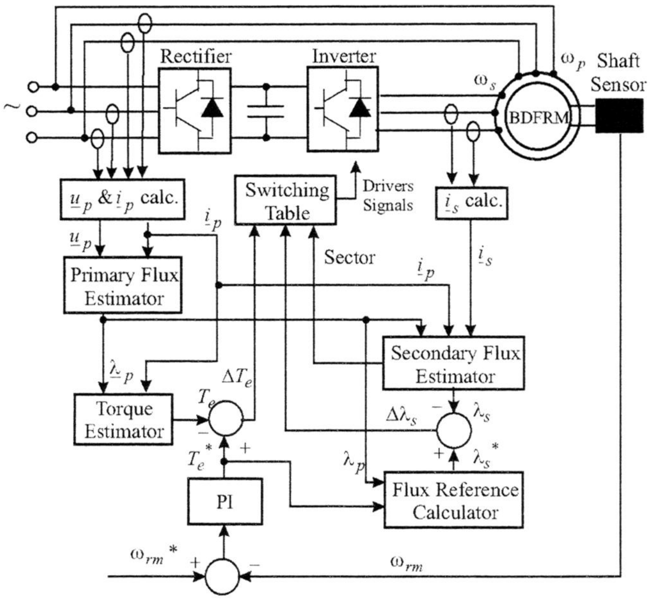


Fig. 1. A simplified diagram of a BDFRM drive with DTC

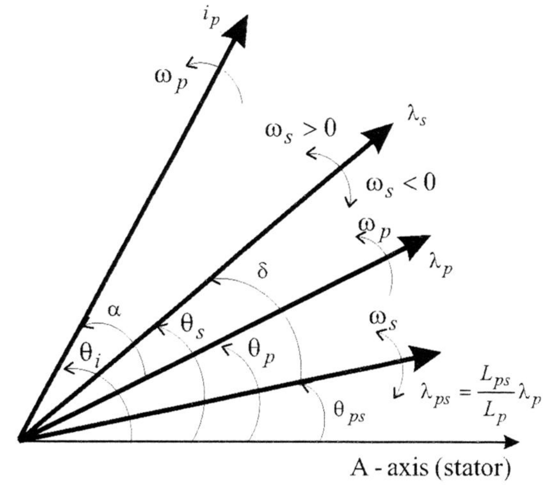


Fig. 2. Characteristic phasors in a stationary reference frame

sub-synchronous mode ($s > 0$ here as with induction motors).

The meaning of the exponential terms in (3) and (4) is extremely important for the proper understanding of the machine unconventional operating principle [8]. These are the 'coupled' flux phasors from the secondary to the primary winding and vice-versa, and they rotate at $\omega_p$ and $\omega_s$ respectively as follows from (ignoring phase angles for convenience of qualitative analysis) [8]:

$$L_{ps}\underline{i}^*_{s,p_s} e^{j\theta_r} = L_{ps} I_{s,p} e^{j(\omega_r-\omega_{s,p})t} = L_{ps} I_{s,p} e^{j\omega_{p,s}t} \quad (6)$$

There is obviously a frequency conversion in the above expression (and not usual turns-ratio referencing from one side to the other as with power transformers or induction machines) which results from the modulation process of the stator mmf waveforms (of different both temporal and spatial pole numbers) via the rotor. This frequency transformation represents the underlaying mechanism of magnetic coupling and torque production in the BDFRM [7, 8].

## III. DTC Strategy

### A. Analogies with Induction Machines

It can be seen that by omitting the differential and $e^{j\theta_r}$ terms in (1)-(4) one obtains equations similar to the DEWRIM in an arbitrary reference frame rotating at $\omega_p$ [8]. The main DTC concepts for the BDFRM can be established from the resulting flux and torque expressions:

$$\underline{\lambda}_p = L_p\underbrace{(i_{pd}+ji_{pq})}_{\underline{i}_p} + L_{ps}\underbrace{(i_{sd}-ji_{sq})}_{\underline{i}_s^*} \quad (7)$$

$$\underline{\lambda}_s = \sigma L_s \underline{i}_s + \underbrace{\frac{L_{ps}}{L_p}\underline{\lambda}_p^*}_{\underline{\lambda}_{ps}} = \sigma L_s(i_{sd}+ji_{sq}) + \underline{\lambda}_{ps} \quad (8)$$

$$T_e = \frac{3p_r}{2\sigma L_s}\left|\underline{\lambda}_{ps}\times\underline{\lambda}_s\right| = \frac{3p_r}{2\sigma L_s}\frac{L_{ps}}{L_p}\lambda_p\lambda_s\sin\delta \quad (9)$$

where $\sigma = 1 - L_{ps}^2/(L_pL_s)$ is the leakage factor (defined as with the induction machine), $\lambda_{ps}$ is the primary flux linking the secondary winding, and $\lambda_s$ is the controllable secondary flux magnitude. The angular positions of these phasors (they both rotate at $\omega_s$ allowing torque to be produced from the machine) are self-evident from Fig.2. Note that $\lambda_p$, and therefore $\lambda_{ps}$, are approximately constant due to the primary winding grid connection.

An immediately obvious conclusion from (1)-(9) is that there is a close modelling link between the BDFRM and the DEWRIM despite the principally distinct operating principle. This convenience means that the fundamental DTC theory for cage induction machines [11, 12] can serve as a benchmark for the DTC development of the BDFRM (Fig. 1) bearing in mind that, in a control sense, $\lambda_{ps}$ and $\lambda_s$ are analogous to the rotor and stator flux of the induction machine respectively. Issues related to this will be addressed in the final paper for space reasons.

The essential difference between the two machines is the possibility of sustained sub-synchronous operation of the BDFRM (the torque and speed are of the same sign i.e. both positive or negative) with the inverter in regenerative mode unlike the cage induction motor which is then under dynamic breaking conditions. In this speed region $\underline{\lambda}_{ps}$ and $\underline{\lambda}_s$ both rotate in the opposite direction to $\underline{\lambda}_p$ (Fig.2) due to the reversed phase sequence of the secondary to the primary winding.

### B. Optimising Secondary Flux

Using (7)-(9) one can derive an expression for determination of the secondary flux reference ($\lambda_s^*$) for a particular optimum performance parameter of the machine and a desired torque ($T_e^*$). For example, the maximum torque per inverter ampere (MTPIA) strategy allows the minimum inverter loading and higher machine efficiency for a given torque [1, 10, 13]. This control objective would be satisfied providing that the secondary current was only participating in the machine torque (and not flux) production. Therefore, by setting $i_{sd} = 0$ in (7)-(9), the corresponding $\lambda_s^*$ can be shown to be:

$$\lambda_s^* = \sqrt{\lambda_{ps}^2 + \left(\frac{\sigma L_{ps}}{1-\sigma}\frac{2T_e^*}{3p_r\lambda_p}\right)^2} \quad (10)$$

Considering that most of the secondary flux comes from the primary side through mutual coupling (represented by $\lambda_{ps} \approx$ const.), the variable torque term in (10) is only a small portion of the $\lambda_s^*$ magnitude. This means that the BDFRM is virtually fully fluxed even when unloaded and, in this respect, its inherently sluggish transient response to load torque changes can be considerably improved making it more competitive with conventional machines. Another important implication of the $\lambda_{ps} \approx$ const. condition is that despite the scalar control nature of the DTC method, the machine performance can still be optimised in a manner similar to vector control but, unlike the latter, in a stationary frame.

### C. Flux and Torque Estimation

The $\lambda_s$ (the flux controller input) and $\theta_s$ (for locating $\underline{\lambda}_s$ position in a stator frame i.e. for sector identification) values (Fig. 2) can be estimated in a traditional way from the measured DC link voltage and knowledge of a particular inverter switching status by applying (2). However, in a narrow range around the synchronous speed ($\omega_{syn} = \omega_p/p_r$), where the machine is normally operated, $\omega_s$ is small and this approach may experience the same voltage integration problems and flux estimation inaccuracies of DTC algorithms for conventional singly-fed machines at low speeds. Since both the BDFRM windings are externally accessible, it is possible to eliminate this well-known DTC deficiency by employing the following relationships (assuming isolated neutral points and 'abc' phase sequence of the Y-connected windings as shown in Fig. 3):

$$\underline{\lambda}_s = \lambda_s e^{j\theta_s} = L_s \underline{i}_s + \frac{\underline{\lambda}_p - L_p \underline{i}_p}{\underline{i}_s^*}\underline{i}_p^* \tag{11}$$

$$\underline{\lambda}_p = \lambda_p e^{j\theta_p} = \int (\underline{u}_p - R_p \underline{i}_p)\, dt \tag{12}$$

$$\underline{i}_x = i_{a_x} + j\frac{i_{a_x} + 2i_{b_x}}{\sqrt{3}}, \qquad x = p, s \tag{13}$$

$$\underline{u}_p = u_{a_p} + j\frac{u_{a_p} + 2u_{b_p}}{\sqrt{3}} \tag{14}$$

where the subscripts 'a' and 'b' denote the respective instantaneous currents and phase voltages. This alternative technique avoids secondary voltage integration but requires knowledge of the winding self inductances $L_{p,s}$ at the expense. The improved control quality is therefore trade-off for the increased parameter dependence in this case. Furthermore, under the MTPIA conditions, for smaller machines (such as the one considered in this paper) having inherently higher resistances, one has to take into account the primary resistance voltage drop in (12). While it is quite true that $R_p i_p << \lambda_p$ in most situations, for the MTPIA control strategy in particular where $i_s$ is a minimum, even minor inaccuracies in $\underline{\lambda}_p$ estimates, when multiplied by a factor of $i_p/i_s$ in (11), can cause large estimation errors in $\underline{\lambda}_s$. Finally, it has been recently demonstrated by the authors [14] that sensorless speed control is also feasible as the rotor 'electrical' angle ($\theta_r = p_r\theta_{rm}$) can be deduced from measurements using (3) and (4).

Amongst different torque expressions for the BDFRM, which are very similar in form to those for induction machines, the best estimates to be used in the torque controller

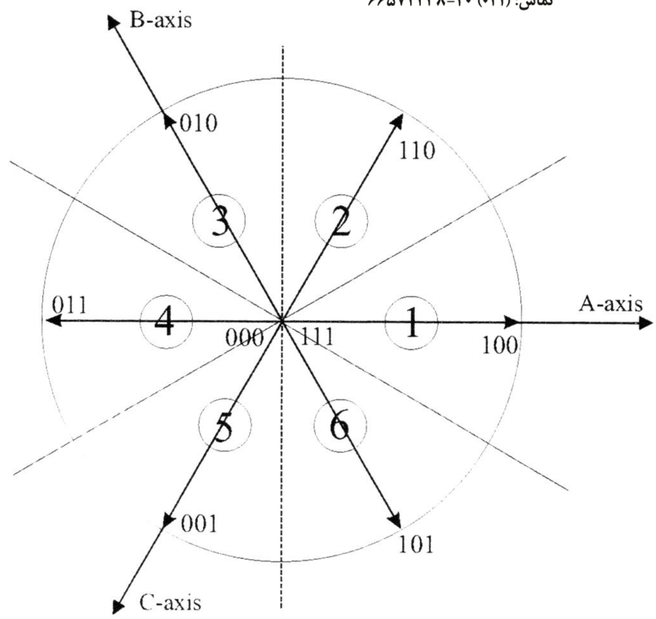


Fig. 3. Secondary voltage vectors and $\pi/3$ sectors

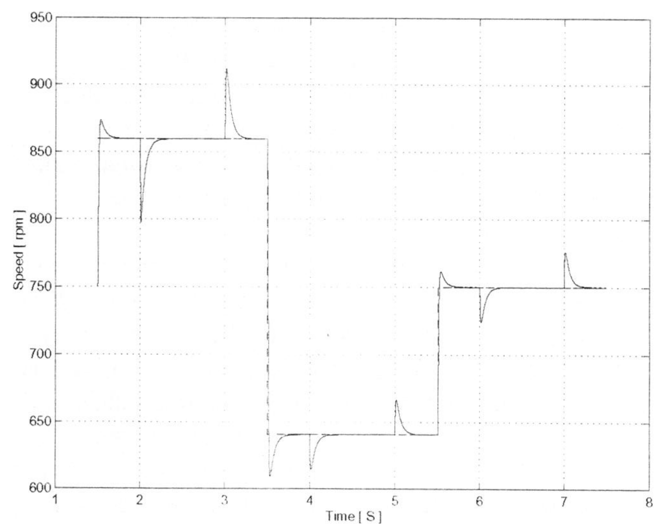


Fig. 4. Machine response to speed/load torque changes

of Fig. 1 can be obtained using:

$$T_e = \frac{3}{2}p_r \left|\underline{\lambda}_p \times \underline{i}_p\right| = \frac{3}{2}p_r \lambda_p i_p \sin\alpha \tag{15}$$

$$= \frac{3}{2}p_r \lambda_p i_p \sin(\theta_i - \theta_p) \tag{16}$$

where $\lambda_p$ and $\theta_p$ are given by (12), and $i_p$ and $\theta_i$ immediately follow from (13). This expression allows high estimation accuracy since it is only dependent on $R_p$ (indirectly through $\lambda_p$) and is exclusively a function of the primary quantities having smooth, virtually 'ripple-free', waveforms at fixed line frequency. Note however that for control strategies other than the MTPIA (in case of smaller machines) and for larger machines in general, where the primary resistance effects are negligible and/or where sensitivity of (11) to $\lambda_p$ estimates is less pronounced, this dependence is extremely weak and can be ignored.

TABLE I
OPTIMUM SWITCHING LOOK-UP TABLE

| Comparator | | Sector | | | | | |
|---|---|---|---|---|---|---|---|
| $\Delta\lambda_s$ | $\Delta T_e$ | 1 | 2 | 3 | 4 | 5 | 6 |
| 1 | 1 | 110 | 010 | 011 | 001 | 101 | 100 |
| 1 | 0 | 101 | 100 | 110 | 010 | 011 | 001 |
| 0 | 1 | 010 | 011 | 001 | 101 | 100 | 110 |
| 0 | 0 | 001 | 101 | 100 | 110 | 010 | 011 |

### D. *Inverter Switching Principles*

The outputs of the flux and torque 2-level comparators in the DTC algorithm for the BDFRM (Fig.1) are:

$$\Delta\lambda_s = \begin{cases} 1, & \lambda_s^* - \lambda_s \geq \Delta\lambda \\ 0, & \lambda_s^* - \lambda_s \leq -\Delta\lambda \end{cases} \quad (17)$$

$$\Delta T_e = \begin{cases} 1, & T_e^* - T_e \geq \Delta T \\ 0, & T_e^* - T_e \leq -\Delta T \end{cases} \quad (18)$$

where $\Delta\lambda$ and $\Delta T$ indicate the respective hysteresis bands, and '1' and '0' mean the increase/decrease respectively of the secondary flux magnitude and/or instantaneous torque in actual (not absolute) sense[4]. The binary codes (with '1' signifying the top device ON and the bottom OFF, and '0' corresponding to the opposite switching states as usual in the literature), and angular positions of the voltage vectors to be applied to the secondary winding to achieve a desired control action with the minimum number of switchings are given in Table I and Fig. 3.

Notice from Table I that only the active switching states of the inverter legs (based on non-zero vectors) have been used for the control. This approach has been chosen because it offers many advantages such as [14]: (a) the DTC scheme becomes simpler and sensorless in nature (the influence of zero vectors, '111' or '000', on the machine torque is different for super- and sub-synchronous operation, and in their presence the torque control would be therefore speed dependent); (b) the synchronous speed performance is much better (since the secondary back-emf is zero, the response would be sluggish with the zero vectors applied as there would be no voltage to drive the current); (c) the real-time implementation is considerably facilitated as the dSPACE® compilers only accept 2-level comparator functional subroutines that are readily available in the Simulink® library (with the zero-vectors included, the torque comparator would have a 3-level structure).

## IV. SIMULATION STUDIES

The following plots have been generated by executing the algorithm in Fig.1 in Simulink® for the MTPIA strategy using the parameters (listed in the Appendix) of a custom designed and built 6/2 pole BDFRM prototype. The machine starting characteristics have been omitted for better scaling in order to focus closely to control aspects only. It should also be mentioned that the circuitry required for starting is not shown in Fig.1. In practice, if a partially rated inverter is used, auxiliary contactors are usually needed to short the secondary terminals directly or through external resistors to allow the BDFRM start as a wound rotor induction machine thus preventing the inverter overloading. Once the machine speed is near synchronous the contactors are opened and the inverter is connected with the control enabled (this occurs at 1.5-s time instant in the simulated plots).

[4]The torque is assumed positive if acting anti-clockwise.

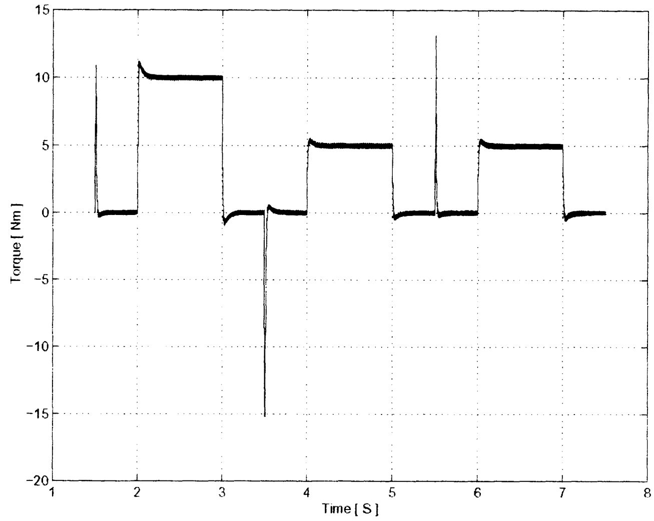


Fig. 5. Machine Torque

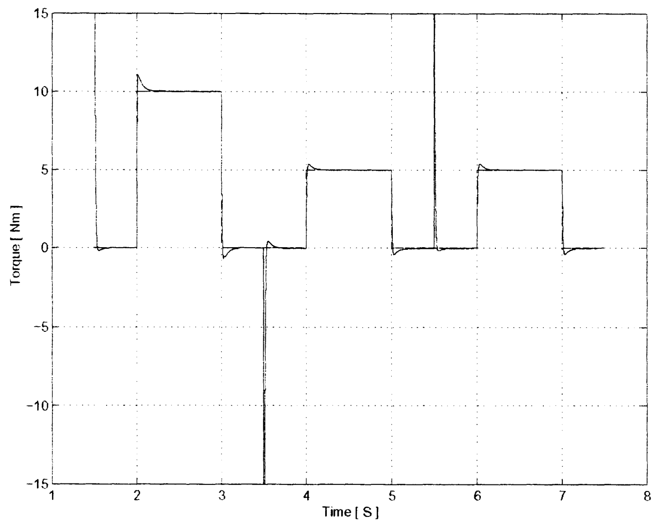


Fig. 6. Desired Torque

Fig.4 shows that the 'theoretical' machine can be effectively controlled in either super-synchronous, synchronous or sub-synchronous mode under different loading conditions. This can be attributed to the accurate torque and flux control (especially in steady-state) within the specified hysteresis bands as can be seen from Figs.5-8.

The machine transient response to speed/load torque step changes is satisfactory. The 'tooth-alike' pulses while loading and unloading the machine, notable in the speed waveform of Fig.4, can be expected from dynamically sluggish PI speed control coupled with inherently limited rate of change of torque of the machine. The magnitude of these 'overshoots' can be alleviated by the more optimal tuning of the PI gains.

## V. Experimental Results

The promising potential and good performance of the algorithm, anticipated by simulations, have just been experimentally verified on a real drive system (see the Appendix for details), but only some results for the unloaded machine (load tests are yet to be conducted) are available at this stage. The plots in Figs.9 and 10 are generated for 20-kHz torque control rate whereas the speed estimates (derived from rotor position measurements using a simple Euler's approximation) are updated at 1-kHz only in order to minimise quantisation errors. Such a high control rate is quite impressive and it means that it takes no more than 50 $\mu$s for the processor to do all control calculations (surely, the variable inverter switching frequency, typical for DTC, is much below this figure).

The speed waveform in Fig.9 clearly shows the BDFRM ability to operate successfully in a limited range above, below and even at synchronous speed (78.54 rad/s = 750 rpm) when the secondary frequency is zero (from about 17-s onward). It is well known that the low frequency operation in general is hardly achievable with many inverter-fed DTC machines, foremost cage induction motors. It should be noted that prior to the control being enabled (at 5-s), the BDFRM was running as a wound rotor induction machine with the short-circuited secondary terminals (the same procedure is also used for the starting). The machine speed in this region is slightly below the synchronous as dictated by the no-load slip. However, notice that, when controlled, the BDFRM operates synchronously, in a manner similar to a conventional inverter-fed synchronous motor, and after about 17-s its speed is exactly synchronous as desired.

The good speed controller performance is a consequence of the quality torque control allowing a desired trajectory to be accurately followed under all operating conditions except while reducing the speed from a super-synchronous to an under-synchronous value as illustrated in Fig. 10. A compromised transient response is clearly visible in the waveforms and is likely due to hardware problems in the DC link chopper circuitry (currently under investigation) this preventing an effective dumping of the breaking power into the regeneration resistors. Finally, notice from Fig. 10 that the electromagnetic torque values are about 5-Nm while the machine is unloaded i.e. with zero shaft torque. This phenomenon comes from the fact that an ideal machine model, neglecting core losses, was used for the control, which resulted in the speed PI controller asking for more torque to be produced from the machine to cover the losses i.e. the torque was overestimated. The no-load tests confirmed this conjecture.

## VI. Conclusions

A DTC scheme for the BDFRM, that is also applicable to the DEWRIM, has been proposed and its effectiveness at different speeds down to zero secondary winding frequency has been verified both by computer simulations and experimentally. In this sense, the BDFRM has been shown to be superior to most machines with DTC.

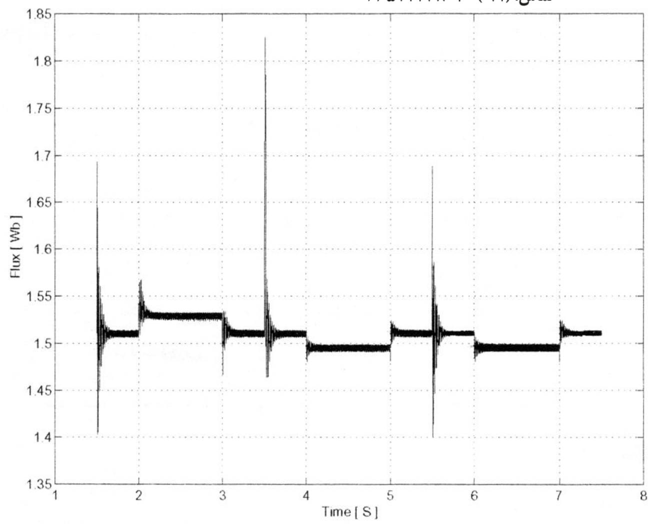


Fig. 7. Secondary Flux

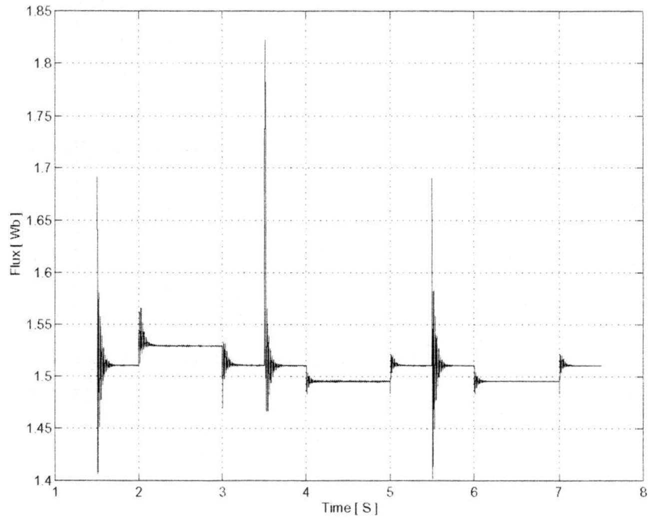


Fig. 8. MTPIA Secondary Flux Reference

## Appendix

## I. BDFRM Test Rig

The laboratory test system for a 1.5 kW, 750 rpm 'proof-of-concept' BDFRM driving an 'off-the-shelf' DC load machine is presented in Fig.11. An IGBT inverter bridge supplying the secondary winding is the 132GDL120-412CTV Semikron® integrated intelligent power (SKiiP) module. The power electronic hardware and machine operation are controlled by a powerful DS1103 PPC controller board of the ACE 1103 CLP DSP development kit from dSPACE®. The TM210 torque transducer, featuring excellent dynamic response suitable for transient testing, is from MAGTROL® whereas a highly precise incremental encoder has been used for shaft position sensing and speed estimation.

The machine inductances used for the control have been obtained by applying standard off-line testing methods for conventional slip ring induction machines largely following the procedure described in [3]. This approach is justified by the close modelling similarities of the two machines as shown in the main text. The actual resistances (measured by

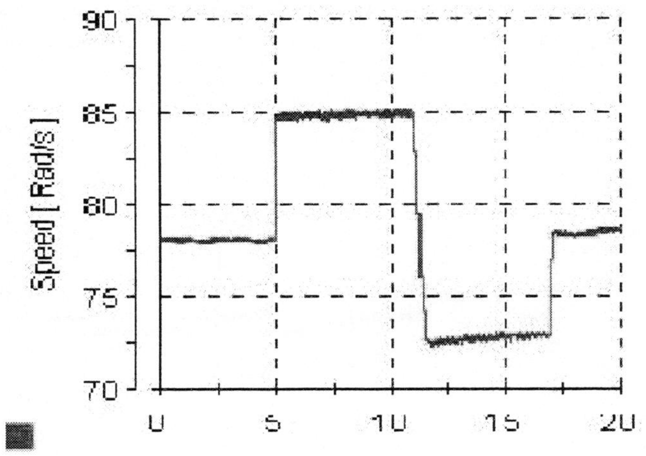


Fig. 9. Experimental Speed Waveform from dSPACE (control activated at 5-s)

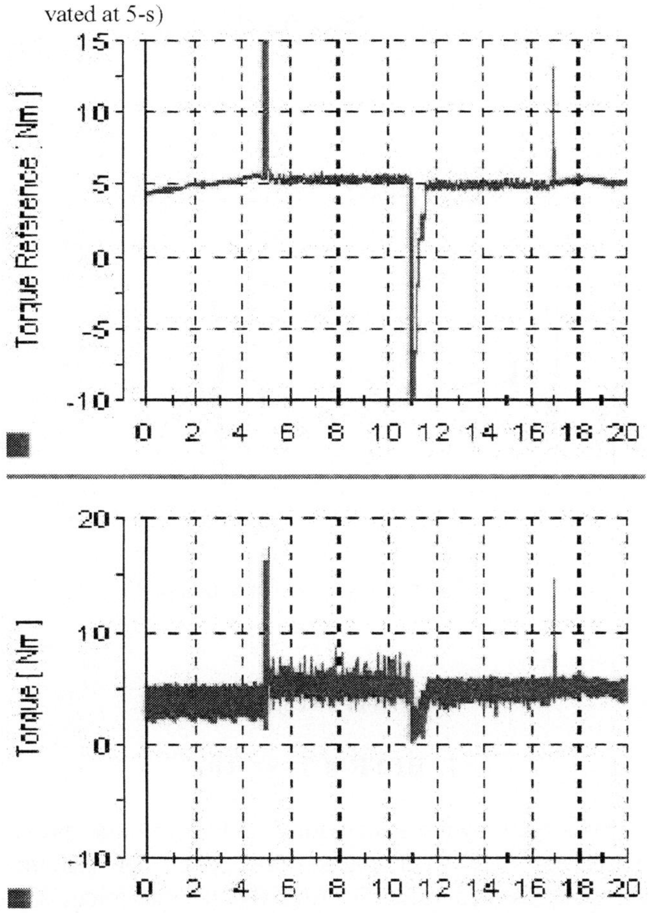


Fig. 10. Desired (top) and estimated torque (bottom) from dSPACE corresponding to results in Fig.9

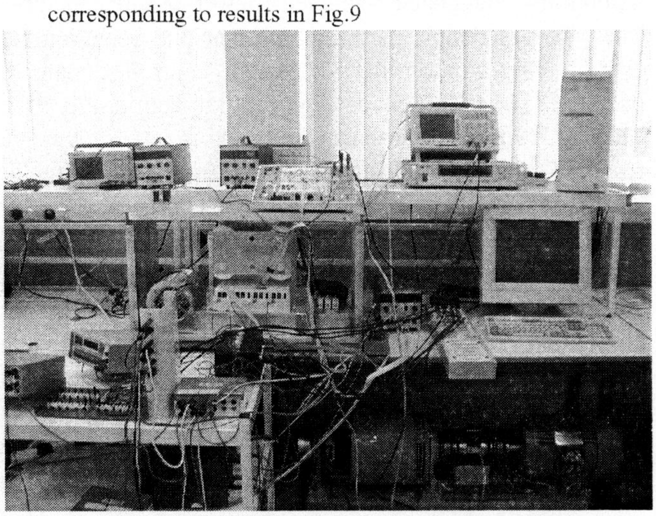

Fig. 11. BDFRM Test System

a simple DC test) and 3-phase inductances of the windings are: $R_p = 10.7\Omega$, $R_s = 12.7\Omega$, $L_p = 0.43$H, $L_s = 1.26$H and $L_{ps} = 0.41$H. The somewhat higher values of the machine parameters are due to a small gage copper wire employed and consequent larger number of turns of the windings (especially the secondary one). Note that the primary and secondary winding sections have been accommodated in the same slots so that there is no space displacement between the respective phase axes.

## References

[1] M.G.Jovanović, R.E.Betz, and J.Yu, "The use of doubly fed reluctance machines for large pumps and wind turbines," *IEEE Transactions on Industry Applications*, vol. 38, pp. 1508–1516, Nov/Dec 2002.

[2] S. Williamson, A. Ferreira, and A. Wallace, "Generalised theory of the brushless doubly-fed machine. part 1: Analysis," *IEE Proc.-Electric Power Applications*, vol. 144, pp. 111–122, March 1997.

[3] F.Wang, F.Zhang, and L.Xu, "Parameter and performance comparison of doubly-fed brushless machine with cage and reluctance rotors," *IEEE Transactions on Industry Applications*, vol. 38, pp. 1237–1243, Sept/Oct 2002.

[4] L. Xu, L. Zhen, and E. Kim, "Field-orientation control of a doubly excited brushless reluctance machine," *IEEE Transactions on Industry Applications*, vol. 34, pp. 148–155, Jan/Feb 1998.

[5] W.R.Brassfi eld, R.Spee, and T.G.Habetler, "Direct torque control for brushless doubly-fed machines," *IEEE Transactions on Industry Applications*, vol. 32, no. 5, pp. 1098–1104, 1996.

[6] S.Arnalte, J.C.Burgos, and J.L.Rodriguez-Amenedo, "Direct torque control of a doubly-fed induction generator for variable speed wind turbines," *Electric power components and systems*, vol. 30, pp. 199–216, 2002.

[7] Y. Liao, L. Xu, and L. Zhen, "Design of a doubly-fed reluctance motor for adjustable speed drives," *IEEE Transactions on Industry Applications*, vol. 32, pp. 1195–1203, Sept/Oct 1996.

[8] R.E.Betz and M.G.Jovanović, "Introduction to the space vector modelling of the brushless doubly-fed reluctance machine," *Electric Power Components and Systems*, vol. 31, pp. 729–755, August 2003.

[9] F. Liang, L. Xu, and T. Lipo, "D-q analysis of a variable speed doubly AC excited reluctance motor," *Electric Machines and Power Systems*, vol. 19, pp. 125–138, March 1991.

[10] R.E.Betz and M.G.Jovanović, "The brushless doubly fed reluctance machine and the synchronous reluctance machine - a comparison," *IEEE Transactions on Industry Applications*, vol. 36, pp. 1103–1110, July/August 2000.

[11] I.Takahashi and T.Noguchi, "A new quick-response and high-effi ciency control strategy of an induction machine," *IEEE Transactions on Industry Applications*, vol. IA-22, pp. 820–827, Sept/Oct 1986.

[12] P. Vas, *Sensorless Vector and Direct Torque Control*. Oxford University Press, 1998, ISBN 0-19-856465-1.

[13] R.E.Betz and M.G.Jovanović, "Theoretical analysis of control properties for the brushless doubly fed reluctance machine," *IEEE Transactions on Energy Conversion*, vol. 17, pp. 332–339, Sept 2002.

[14] M.G.Jovanović, J.Yu, and E.Levi, "A doubly-fed reluctance motor drive with sensorless direct torque control," *IEEE International Electric Machines and Drives Conference (IEMDC)*, Madison, Wisconsin, June 2003.